

New Limits on Coherent Neutrino Nucleus Elastic Scattering Cross Section at the Kuo-Sheng Reactor Neutrino Laboratory

S. Karmakar,^{1,2,*} M.K. Singh,^{1,3,†} V. Sharma,^{1,4} H.T. Wong,^{1,‡} Greeshma C.,^{1,5} H.B. Li,¹ L. Singh,^{1,5} M. Agartioglu,^{1,6,7} J.H. Chen,¹ C.I. Chiang,¹ M. Deniz,⁶ H.C. Hsu,¹ S. Karadağ,^{1,8} V. Kumar,^{1,2} C.H. Leung,¹ J. Li,⁹ F.K. Lin,¹ S.T. Lin,¹⁰ S.K. Liu,¹⁰ H. Ma,⁹ K. Saraswat,¹ M.K. Singh,² V. Singh,^{5,3} D. Tanabe,¹ J.S. Wang,¹ L.T. Yang,⁹ C.H. Yeh,¹ and Q. Yue⁹

(TEXONO Collaboration)

¹*Institute of Physics, Academia Sinica, Taipei 11529*

²*Department of Physics, Institute of Applied Sciences and Humanities, GLA University, Mathura 281406*

³*Department of Physics, Institute of Science, Banaras Hindu University, Varanasi 221005*

⁴*Department of Physics, H.N.B. Garhwal University, Srinagar, Uttarakhand-246174*

⁵*Department of Physics, School of Physical and Chemical Sciences, Central University of South Bihar, Gaya 824236*

⁶*Department of Physics, Dokuz Eylul University, Buca, İzmir 35160*

⁷*Department of Physics, National Dong Hwa University, Shoufeng, Hualien 97401*

⁸*Department of Physics Engineering, Istanbul Technical University, Sarıyer, Istanbul 34467*

⁹*Department of Engineering Physics, Tsinghua University, Beijing 100084*

¹⁰*College of Physics, Sichuan University, Chengdu 610065*

(Dated: April 8, 2025)

Neutrino nucleus elastic scattering (νA_{el}) with partial quantum-mechanical coherency has been observed in several nuclei with neutrinos from decay-at-rest pions. This interaction with reactor neutrinos where coherency is $>95\%$ has not yet been experimentally observed. We present new results on the studies of νA_{el} cross section with an electro-cooled p-type point-contact germanium detector at the Kuo-Sheng Reactor Neutrino laboratory. A total of 242(357) kg-days of Reactor ON(OFF) data at a detector threshold of 200 eV in ionization energy are analyzed. The Lindhard model parametrized by a single variable k which characterizes the quenching function was used. Limit at 90% confidence level of $\rho < 4.7$ at the predicted value of $k=0.162$ is derived, where ρ is the ratio of the measured to standard model (SM) cross section. Conversely, $k < 0.288$ at the SM-value of $\rho=1$.

The elastic scattering of neutrinos with a nucleus $A(Z, N)$ (denoted by νA_{el} , also represented as $CE\nu NS$ in the literature) [1, 2]:

$$\nu + A(Z, N) \rightarrow \nu + A(Z, N) \quad (1)$$

is a fundamental electroweak neutral current process in the Standard Model (SM). Its cross section at low momentum transfer (q^2) is increased by quantum-mechanical coherency effects relative to those of other neutrino interactions. At typical reactor neutrino energy (E_ν) where individual nucleon effects can be ignored, the differential and total cross sections for νA_{el} can be approximated [3] by, respectively:

$$\left[\frac{d\sigma}{dq^2} \right] \approx \frac{N^2}{2} \left[\frac{G_F^2}{4\pi} \right] \left[1 - \frac{q^2}{4E_\nu^2} \right] \quad \text{and} \quad (2)$$

$$\sigma \approx N^2 \left[\frac{G_F^2 E_\nu^2}{4\pi} \right]$$

showing an enhancement by N^2 , the neutron number squared. Studies of νA_{el} [4, 5] can provide sensitive probes to physics beyond the SM (BSM), various astrophysical processes, and the neutron density distributions. It can be applied to supernova neutrino detection and real-time monitoring of nuclear reactors with compact and transportable neutrino detectors. There are several

active experimental programs on νA_{el} , with neutrinos from reactors or from decay-at-rest pions (DAR- π) provided by spallation neutron source [6].

First measurement of νA_{el} was achieved with DAR- π - ν in the COHERENT experiment with CsI(Na) scintillator [7], followed by measurements with liquid Ar [8] and Ge detectors [9]. The νA_{el} events from solar and atmospheric neutrinos are the irreducible “neutrino fog” background in dark matter experiments [10]. First hints of observation of νA_{el} in solar neutrinos are recently reported [11, 12].

The coherency effects of DAR- π - ν , which can be quantitatively characterized by parameter α [3, 13], are only partial and incomplete ($\alpha \sim 14\% - 51\%$). These deviations from the perfect coherency case ($\alpha=1$) would have to be described and quantified before νA_{el} can be effectively applied towards other goals like sensitive BSM searches. Reactor νA_{el} , on the other hand, would typically have $\alpha > 95\%$ due to lower q^2 . The nuclear recoil energy, however, is less than a few keV which translates to the measurable ionization energy of $T < 500$ eV in germanium (Ge) detectors. This poses severe constraints to the detector requirements.

Studies of reactor νA_{el} are actively pursued in several experiments. Ge ionization detectors have the merits of being a mature technology with relatively large modu-

lar mass, low detection threshold and low intrinsic background. Ge-detectors with sub-keV sensitivities were first used in the TEXONO light Dark Matter [14] and νA_{el} program [15], which evolved to the adoption of the p-type Point-Contact Ge-detectors (pPCGe) [16–19]. Subsequent reactor νA_{el} experiments using pPCGe include CONUS [20–23], DRESDEN-II [24] and ν GEN [25]. The pursuit of reactor νA_{el} with pPCGe catalyzed the CDEX Dark Matter program at the China Jinping Underground Laboratory [26].

The TEXONO research program [27] conducts experiments at the Kuo-Sheng Reactor Neutrino Laboratory (KSNL) [28–31]. The laboratory has an overburden of about 30 meter-water-equivalence and is located at a distance of 28 m from Core No.1 of KSNL with a nominal thermal power output of 2.9 GW. The shielding design is realized with 50 tons of materials including, from outside in, plastic scintillator panels for cosmic-ray (CR) vetos, 15 cm of lead, 5 cm of stainless steel structure, 25 cm of boron-loaded polyethylene and 5 cm of oxygen free highly conducting copper. Subject-specific experimental configurations are placed into an inner space with dimension of 60 cm \times 100 cm \times 75 cm (height). Details of the facility are documented in previous publications [28, 29].

This analysis is based on data taken at KSNL from December 2020 to January 2023 with a pPCGe [32] enclosed by an Anti-Compton (AC) detector made of NaI(Tl) scintillating crystal [28]. The target sensor is a Ge-crystal with diameter 70 mm and height 70 mm and a mass of 1434 g. There are two novel features of this “Generation-3 (G3)” detectors relative to earlier ones: (i) electro-cooling of the Ge-sensors [33, 34] and (ii) improved front-end electronics design. In addition, “pulser” events are recorded for various control and calibration purposes. These are signals generated with programmable rise-times optimized to match those of the intrinsic 10.37 keV cosmogenic peak due to ^{68}Ge , and with amplitudes adjusted to match the respective energy values [21, 35].

Detector threshold for physics analysis is crucial in the studies of reactor νA_{el} . This is characterized by two measurables: (i) the resolution in full-width-half-maximum (FWHM) with pulser events, and (ii) the “noise-edge” below which energy the electronic pedestal noise would dominate the event rates. The achieved pulser FWHM is 70.2 eV and the noise-edge is 200 eV for the G3 detectors. These improves over previous generations of pPCGe with pulser FWHM at 150 eV and 122 eV and noise-edge at 500 eV and 300 eV [19, 30, 31, 36].

Stability of the root-mean-square pedestal noise (σ_{ped}) behavior is crucial for this long duration data taking, and is illustrated in Figure 1a. The power consumption for the electro-cooler is superimposed, showing that its inevitable variations have no effects on the pedestal stability. Following the noise-edge versus σ_{ped} behavior depicted in Figure 12a of Ref. [19], the residual fluctua-

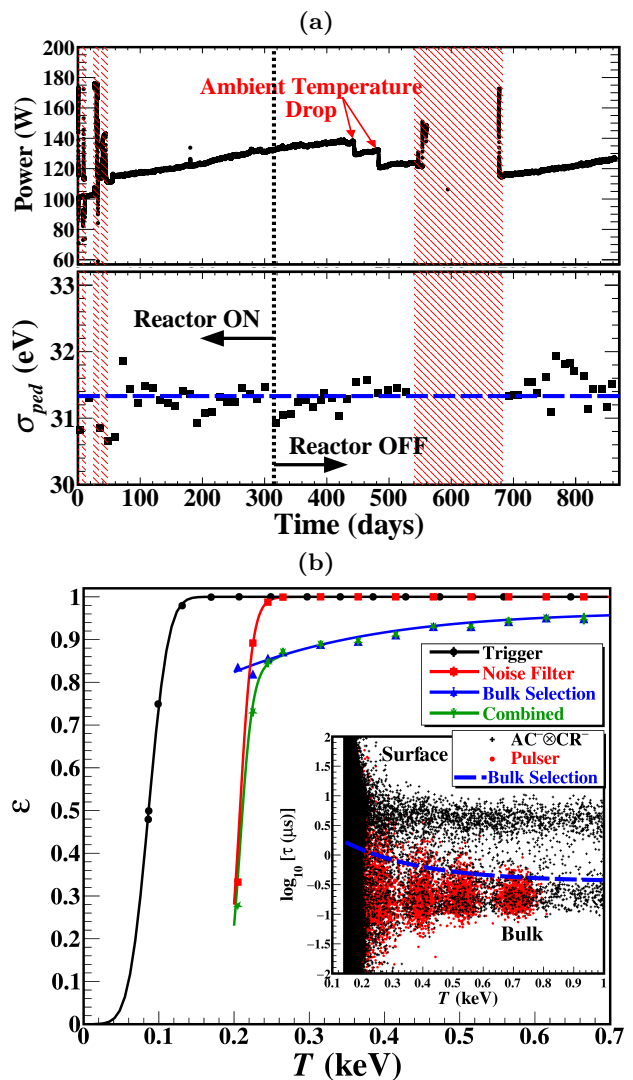


FIG. 1. (a) Power consumption by the electro-cooler of pPCGe and the pedestal noise σ_{ped} during data taking, showing σ_{ped} is stable and uncorrelated to the cooler operation. Shaded bands are suspended periods of data taking. All structures of the cryo-cooler power evolution are due to understood hardware or ambient conditions. (b) Measured signal efficiencies due to trigger conditions, pedestal noise filters and B-Selection. The τ -distributions for physics and pulser events, as well as the B(S) selection contour, are displayed in the inset. The T -independent efficiencies are listed in Table I.

tations of <0.5 eV corresponds to effective change of physics noise-edge of <3.5 eV, well within one energy bin in analysis.

A data acquisition trigger is produced via a discriminator threshold to the pPCGe pulse at 6 μs shaping time. The trigger efficiency measured with pulser signals is displayed in Figure 1b. After straightforward data quality filters, a total of (242)357 kg-days Reactor ON(OFF) data are analyzed. Valid events are placed into eight categories according to their CR, AC and B(S) signatures,

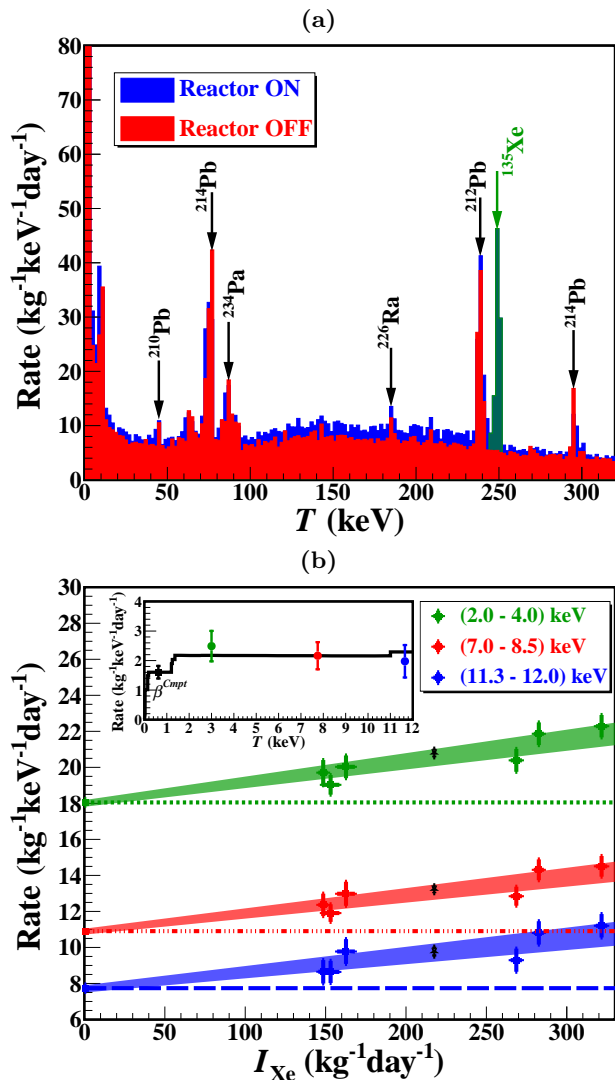


FIG. 2. (a) Measured high energy νA_{el} -candidate spectra of pPCGe during Reactor ON and OFF, showing the ON-only 249.8 keV γ -line due to ^{135}Xe . (b) The correlation between the constant background rates in three different energy bands without cosmogenic X-ray peaks with the intensity (I_{Xe}) of the ^{135}Xe γ -line. The intercepts at $I_{\text{Xe}}=0$ correspond to the accurately-measured Reactor OFF rates. The shaded region denotes the $\pm 1\sigma$ uncertainty bands and the black points correspond to the measured values of the combined data. The predicted Compton background [37] fixed by the rates of the three bands is depicted in the inset.

where $B(S)$ is the bulk-versus-surface events differentiation. Signal selection by CR and AC vetos are applied, so that the survived νA_{el} -candidate events are in anti-coincidence to the other detector components. The $B(S)$ events are identified by their fast(slow) τ via pulse shape discrimination techniques [19, 38, 39]. This is illustrated in the inset of Figure 1b. Signal efficiencies are derived by the survival of pulser events under the same selection procedures. The surface layer thickness is ≤ 0.5 mm [32] and the fiducial mass is 1383 g.

TABLE I. Summary of T -independent signal selection efficiencies. The T -dependent components are displayed in Figure 1b.

Signal Selection	Efficiency (%)
Data Acquisition	99.77
Basic Data Quality	99.64
Cosmic-Ray Veto CR ⁻	88.57
Anti-Compton Veto AC ⁻	99.84
Combined	87.91

The non- νA_{el} background events are important: (i) to provide efficiency measurements on the various selection procedures, (ii) as stability monitors, and (iii) as tuning samples for parameter optimization in the analysis algorithms. The energy-independent signal detection efficiencies through the data acquisition and analysis procedures are summarized in Table I. The energy-dependent efficiencies from pedestal noise filters and BS selection is depicted in Figure 1b. The analysis procedures follow closely the scheme established by previous pPCGe experiments described in Refs. [19, 28, 38, 39].

Anomalous Reactor ON related background due to ^{135}Xe contamination is observed in this data set. The isotope ^{135}Xe [40] is a fission product and undergoes β -decay at a half-life of 9.14 hour to $^{135}\text{Cs}^*$ which decays promptly by γ -rays emissions to the long-lived ^{135}Cs ground state. As displayed in Figure 2a, the signature γ -line at 249.8 keV is measured in the Reactor ON spectra, at a rate of $I_{\text{Xe}}=(218\pm 2)$ kg⁻¹day⁻¹ from which observable features at low energy are produced. This is much higher than that in our earlier experiment at KSNL [28], in which $I_{\text{Xe}}=(11.6\pm 0.5)$ kg⁻¹day⁻¹. The main cause of the increase is the use of electro-cooling in pPCGe which replaces purging of the inner volume with the boil-off of liquid nitrogen from conventional dewar.

The Compton continuum background is linearly correlated with I_{Xe} . This is illustrated in Figure 2b for the 2-4 keV, 7-8.5 keV, and 11.3-12 keV energy regions. The averaged rates of the three bands (black data-points) show consistent excess over their respective Reactor OFF $I_{\text{Xe}}=0$ levels, confirming that high energy ambient γ -rays produce Compton background to the νA_{el} -candidate samples in the low energy (<10 keV) region. The spectrum is flat but with step-wise structures at atomic transition energies. There are no other ON-only ambient background sources besides ^{135}Xe , whose event rate is only $<1.5\%$ of the Reactor ON background at the low energy <300 eV region. This background can be accounted for and subtracted.

The reactor $\bar{\nu}_e$ -spectrum is adopted from that derived in Ref. [28]. The total $\bar{\nu}_e$ -flux is fixed by the reactor thermal power output and corresponds to 6.35×10^{12} cm⁻²s⁻¹. A conservative uncertainty of 5% is assigned, at a comparable range with those of similar experiments [24, 41].

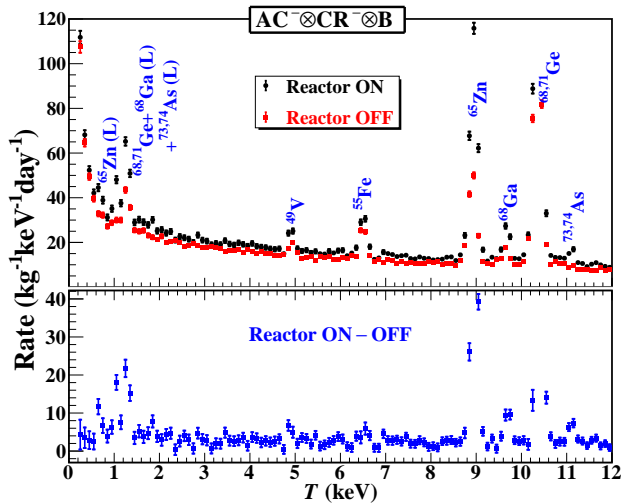


FIG. 3. (Top) Candidate νA_{eI} spectra from 242(357) kg-days of Reactor ON(OFF) data. The cosmogenic X-ray lines are identified. (Bottom) Reactor ON–OFF spectrum showing the finite ^{135}Xe Compton excess. Cosmogenic peaks are observed for those isotopes with half-lives comparable to the data taking duration. The 10.37 keV X-ray peak extends off-scale and is truncated for clarity in display.

As will be shown in what follows, while the neutrino flux is the leading systematic error in this analysis, it is negligible compared to the measurement statistical uncertainties. The Reactor ON/OFF and ON–OFF spectra for the νA_{eI} -candidate events at the low energy (<12 keV) regions are shown in Figure 3. The constant excess in the ON–OFF spectrum is from Compton background events due to γ 's from ^{135}Xe . Its mean rate ($\beta^{Cmpt}=1.61 \text{ keV}^{-1}\text{kg}^{-1}\text{day}^{-1}$) and uncertainty ($\Delta^{Cmpt}=0.21 \text{ keV}^{-1}\text{kg}^{-1}\text{day}^{-1}$) at 200 eV are derived using the Compton spectrum modeling of Ref. [37] and the best-fit ON–OFF measured background levels of the three energy ranges displayed in Figure 2b.

Nuclear recoils are produced in νA_{eI} and a “quenching function” is necessary to translate this into the measurable energy deposition in Ge. The benchmark Lindhard Model [42] characterized by a single parameter k is adopted in this analysis. The best estimate of $k=(0.162\pm 0.003)$ is derived from existing data [19, 43, 44]. The anomalous low energy data of Ref. [45] with iron-filtered neutron are excluded by the results of Ref. [23] while that with photo-neutron sources are in tension with the recent measurements of Refs. [44, 46]. They are therefore not adopted in this analysis. A χ^2 -analysis is applied to the the signal region of 200–400 eV at bin-size of 10 eV as a function of k :

$$\chi^2(\rho, \beta; k) = \sum_i \left[\frac{N_i - \rho \nu_i^{\text{SM}}(k) - \beta}{\Delta_i} \right]^2 + \left[\frac{\beta - \beta^{Cmpt}}{\Delta^{Cmpt}} \right]^2, \quad (3)$$

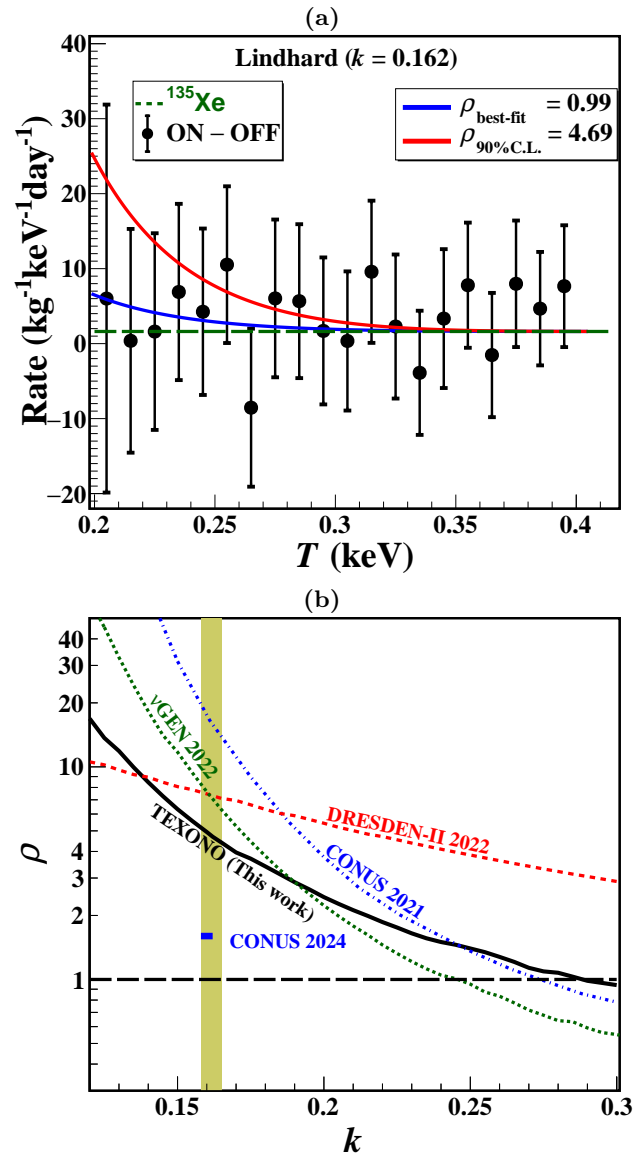


FIG. 4. (a) The ON–OFF νA_{eI} -candidate spectrum at the relevant energy range. Superimposed are the best-fit and 90% C.L. upper limit spectra at $k=0.162$ for Lindhard model. The constant ^{135}Xe -induced background is depicted by the dashed line. (b) Exclusion plot of ρ versus k in νA_{eI} at 90% C.L. The $\pm 3\sigma$ interval on k is represented by the shaded band. Other reactor limits with pPCGe from CONUS [20, 23], DRESDEN-II [24] and νGeN [25] are superimposed.

where the N_i (Δ_i) are the counts (uncertainties) of the i^{th} data point of ON–OFF spectrum, $\nu_i^{\text{SM}}(k)$ is the SM event rate at Lindhard- k . The two outputs are: the best-fit estimate of the ^{135}Xe level (β) and the ratio of the experimental cross section relative to that of SM νA_{eI} (ρ). Depicted in Figure 4a are the ON–OFF spectrum with the best-fit results and the 90% confidence level (C.L.) upper limit at $k=0.162$ derived by the unified approach [47, 48]. The increased error bar at the threshold of 200 eV is due to the drop in signal efficiency shown

in Figure 1b. Figure 4b depicts the exclusion plot at 90% C.L. in ρ versus k , together with the constraints from the other reactor pPCGe experiments: the published CONUS results [20, 23], as well as those from DRESDEN-II [24] and ν GeN [25] data derived via the same analysis procedures.

The best estimate of the ^{135}Xe ON-only background at 200 eV is $\beta=(1.62\pm 0.22)\text{ keV}^{-1}\text{kg}^{-1}\text{day}^{-1}$. The uncertainty is small relative to that of the measured spectrum of $4.26\text{ keV}^{-1}\text{kg}^{-1}\text{day}^{-1}$ within the interval of 200–280 eV which contains 90% of the νA_{el} signals in this analysis. The effects of this background are therefore minor at the present level of sensitivity. Improved sensitivities at $k=0.162$ of $\rho=[0.99\pm 2.23(stat.)\pm 0.05(sys.)]$ as the best-fitted value and $\rho<4.7$ as the 90% C.L. upper limit were derived. Alternatively, in the case where νA_{el} has SM cross section at $\rho=1.0$, then $k<0.288$ at 90% C.L. We note also that the CONNIE reactor νA_{el} experiment with CCD sensors (silicon) has provided a 95% C.L. upper limit of $\rho<76$ [49].

We report in this Letter a new limit on reactor νA_{el} measurement at KSNL which shows an improved sensitivity towards the goal of observation. More data with comparable exposure were taken but under sub-optimal conditions during the COVID-pandemic lockdown periods. Efforts are being made to recover these for physics analysis. We continue to explore advanced pulse shape analysis software techniques with objectives on reducing uncertainties in the bulk-surface event differentiation as well as pushing on the analysis threshold. The next generation ‘‘G4’’ pPCGe detectors are expected to have the sensitivities of <50 eV in pulser FWHM and <150 eV in physics noise-edge, offering the exciting prospects of positive νA_{el} observation at reactors. All reactor cores of KSNL were decommissioned by March 2023. Our νA_{el} program will continue at the new Sanmen Reactor Laboratory under construction in Zhejiang, China [50].

Notes added after completion of this work: the CONUS+ experiment reports preliminary results of observing a 3.7σ signature of the νA_{el} process at power reactor [51].

This work is supported by the Investigator Award AS-IA-106-M02 and Thematic Project AS-TP-112-M01 from the Academia Sinica, Taiwan, and contracts 106-2923-M-001-006-MY5, 107-2119-M-001-028-MY3 and 110-2112-M-001-029-MY3, 113-2112-M-001-053-MY3 from the National Science and Technology Council, Taiwan.

* Corresponding Author: skarmakar@gate.sinica.edu.tw

† Corresponding Author: manu@gate.sinica.edu.tw

‡ Corresponding Author: htwang@phys.sinica.edu.tw

- [1] D. Z. Freedman, Coherent effects of a weak neutral current, *Phys. Rev. D* **9**, 1389 (1974).
 [2] D. Z. Freedman, D. N. Schramm, and D. L. Tubbs, The

weak neutral current and its effects in stellar collapse, *Annual Review of Nuclear and Particle Science* **27**, 167 (1977).

- [3] S. Kerman, V. Sharma, M. Deniz, H. T. Wong, J. W. Chen, H. B. Li, S. T. Lin, C. P. Liu, and Q. Yue (TEXONO), Coherency in Neutrino-Nucleus Elastic Scattering, *Phys. Rev. D* **93**, 113006 (2016), arXiv:1603.08786 [hep-ph].
 [4] M. Abdullah *et al.*, Coherent elastic neutrino-nucleus scattering: Terrestrial and astrophysical applications, (2022), and references therein, arXiv:2203.07361 [hep-ph].
 [5] M. Cadeddu, F. Dordei, and C. Giunti, A view of coherent elastic neutrino-nucleus scattering, *Europhysics Letters* **143**, 34001 (2023), and references therein.
 [6] K. Scholberg, Prospects for measuring coherent neutrino-nucleus elastic scattering at a stopped-pion neutrino source, *Phys. Rev. D* **73**, 033005 (2006), and references therein.
 [7] D. Akimov *et al.* (COHERENT), Observation of Coherent Elastic Neutrino-Nucleus Scattering, *Science* **357**, 1123 (2017), and Supplemental Material, arXiv:1708.01294 [nucl-ex].
 [8] D. Akimov *et al.* (COHERENT Collaboration), First measurement of coherent elastic neutrino-nucleus scattering on argon, *Phys. Rev. Lett.* **126**, 012002 (2021).
 [9] S. Adamski *et al.*, First detection of coherent elastic neutrino-nucleus scattering on germanium, (2024), arXiv:2406.13806 [hep-ex].
 [10] S. Navas *et al.* (Particle Data Group Collaboration), Review of particle physics, *Phys. Rev. D* **110**, 030001 (2024), review on Dark Matter, Section 27 and references therein.
 [11] Z. Bo *et al.* (PandaX Collaboration), First Indication of Solar ^8B Neutrinos through Coherent Elastic Neutrino-Nucleus Scattering in PandaX-4T, *Phys. Rev. Lett.* **133**, 191001 (2024).
 [12] E. Aprile *et al.* (XENON Collaboration), First Indication of Solar ^8B Neutrinos via Coherent Elastic Neutrino-Nucleus Scattering with XENONnT, *Phys. Rev. Lett.* **133**, 191002 (2024).
 [13] V. Sharma *et al.* (TEXONO), Studies of quantum-mechanical coherency effects in neutrino-nucleus elastic scattering, *Phys. Rev. D* **103**, 092002 (2021), arXiv:2010.06810 [hep-ex].
 [14] S. T. Lin *et al.* (TEXONO), New limits on spin-independent and spin-dependent couplings of low-mass WIMP dark matter with a germanium detector at a threshold of 220 eV, *Phys. Rev. D* **79**, 061101 (2009), arXiv:0712.1645 [hep-ex].
 [15] H. T. Wong, H.-B. Li, J. Li, Q. Yue, and Z.-Y. Zhou, Research program towards observation of neutrino-nucleus coherent scattering, *J. Phys. Conf. Ser.* **39**, 266 (2006), arXiv:hep-ex/0511001.
 [16] P. Luke, J. Beeman, F. Goulding, S. Labov, and E. Silver, Calorimetric ionization detector, *Nucl. Instrum. Meth. A* **289**, 406 (1990).
 [17] C. E. Aalseth *et al.* (CoGeNT Collaboration), Experimental constraints on a dark matter origin for the dama annual modulation effect, *Phys. Rev. Lett.* **101**, 251301 (2008).
 [18] C. E. Aalseth *et al.* (CoGeNT Collaboration), Results from a search for light-mass dark matter with a p -type point contact germanium detector, *Phys. Rev. Lett.* **106**,

- 131301 (2011).
- [19] A. Soma *et al.*, Characterization and performance of germanium detectors with sub-keV sensitivities for neutrino and dark matter experiments, *Nucl. Instrum. Meth. A* **836**, 67 (2016).
- [20] H. Bonet *et al.* (CONUS Collaboration), Constraints on elastic neutrino nucleus scattering in the fully coherent regime from the conus experiment, *Phys. Rev. Lett.* **126**, 041804 (2021).
- [21] H. Bonet *et al.*, Pulse shape discrimination for the CONUS experiment in the keV and sub-keV regime, *Eur. Phys. J. C* **84**, 139 (2024), [arXiv:2308.12105 \[physics.ins-det\]](#).
- [22] N. Ackermann *et al.* (CONUS+), The CONUS+ experiment, (2024), [arXiv:2407.11912 \[hep-ex\]](#).
- [23] N. Ackermann *et al.* (CONUS Collaboration), Final CONUS Results on Coherent Elastic Neutrino-Nucleus Scattering at the Brokdorf Reactor, *Phys. Rev. Lett.* **133**, 251802 (2024).
- [24] J. Colaresi, J. I. Collar, T. W. Hossbach, C. M. Lewis, and K. M. Yocum, Measurement of coherent elastic neutrino-nucleus scattering from reactor antineutrinos, *Phys. Rev. Lett.* **129**, 211802 (2022).
- [25] I. Alekseev *et al.* (ν GeN collaboration), First results of the ν GeN experiment on coherent elastic neutrino-nucleus scattering, *Phys. Rev. D* **106**, L051101 (2022).
- [26] J.-P. Cheng *et al.*, The China Jinping Underground Laboratory and its Early Science, *Ann. Rev. Nucl. Part. Sci.* **67**, 231 (2017), [arXiv:1801.00587 \[hep-ex\]](#).
- [27] H. T.-K. Wong, Taiwan EXperiment On Neutrino — History and Prospects, *Int. J. Mod. Phys. A* **33**, 1830014 (2018), [arXiv:1608.00306 \[hep-ex\]](#).
- [28] H. T. Wong *et al.* (TEXONO Collaboration), Search of neutrino magnetic moments with a high-purity germanium detector at the kuo-sheng nuclear power station, *Phys. Rev. D* **75**, 012001 (2007).
- [29] M. Deniz *et al.* (TEXONO Collaboration), Measurement of $\bar{\nu}_e$ -electron scattering cross section with a csi(tl) scintillating crystal array at the kuo-sheng nuclear power reactor, *Phys. Rev. D* **81**, 072001 (2010).
- [30] H. B. Li *et al.* (TEXONO), Limits on spin-independent couplings of WIMP dark matter with a p-type point-contact germanium detector, *Phys. Rev. Lett.* **110**, 261301 (2013), [arXiv:1303.0925 \[hep-ex\]](#).
- [31] L. Singh *et al.* (TEXONO Collaboration), Constraints on millicharged particles with low-threshold germanium detectors at kuo-sheng reactor neutrino laboratory, *Phys. Rev. D* **99**, 032009 (2019).
- [32] Mirion Technologies, Lingolsheim, France, and Manual Specifications.
- [33] Cryo-Pulse 5 Plus, Electrically Refrigerated Cryostat, ([Online Information](#)).
- [34] A. T. A. M. de Waele, Basic Operation of Cryocoolers and Related Thermal Machines, *Journal of Low Temperature Physics* **164**, 179 (2011).
- [35] J.-S. Wang, M. K. Singh, H.-B. Li, and H. T.-K. Wong, Bulk-Surface Event Discrimination in Point Contact Germanium Detectors at Near-Threshold Energies with Shape-Matching Pulse-Shape Methods, (2024), [arXiv:2412.00089 \[physics.ins-det\]](#).
- [36] M. K. Singh, L. Singh, M. Agartioglu, V. Sharma, V. Singh, and H. T. King Wong, Constraints on bosonic dark matter with low threshold germanium detector at kuo-sheng reactor neutrino laboratory, *Chinese Journal of Physics* **58**, 63 (2019).
- [37] C.-K. Qiao, H.-C. Chi, S.-T. Lin, P. Gu, S.-K. Liu, and C.-J. Tang, Compton scattering energy spectrum for Si and Ge systems, *Journal of Physics G: Nuclear and Particle Physics* **47**, 045202 (2020).
- [38] H. B. Li *et al.* (TEXONO), Differentiation of Bulk and Surface Events in p-type Point-Contact Germanium Detectors for Light WIMP Searches, *Astropart. Phys.* **56**, 1 (2014), [arXiv:1311.5957 \[physics.ins-det\]](#).
- [39] L. T. Yang *et al.*, Bulk and Surface Event Identification in p-type Germanium Detectors, *Nucl. Instrum. Meth. A* **886**, 13 (2018), [arXiv:1611.03357 \[physics.ins-det\]](#).
- [40] Q. Li, S. Wang, H. Jia, Y. Fan, X. Zhang, Z. Chen, Y. Zhao, Y. Chang, and S. Liu, Determination of the emission probability of the principal gamma ray of ^{135}Xe , *Nucl. Instrum. Meth. A* **705**, 117 (2013).
- [41] G. Fernandez Moroni, J. Estrada, E. E. Paolini, G. Cancelo, J. Tiffenberg, and J. Molina, Charge coupled devices for detection of coherent neutrino-nucleus scattering, *Phys. Rev. D* **91**, 072001 (2015).
- [42] J. Lindhard, Influence of crystal lattice on motion of energetic charged particles, *Kongel. Dan. Vidensk. Selsk., Mat.-Fys. Medd.* **34**, (1965).
- [43] J. Lindhard, V. Nielsen, M. Scharff, and P. V. Thomsen, Integral equations governing radiation effects. (notes on atomic collisions, iii), *Kgl. Danske Videnskab., Selskab. Mat. Fys. Medd.* **33**, (1963).
- [44] A. Bonhomme *et al.*, Direct measurement of the ionization quenching factor of nuclear recoils in germanium in the keV energy range, *Eur. Phys. J. C* **82**, 815 (2022), [arXiv:2202.03754 \[physics.ins-det\]](#).
- [45] J. I. Collar, A. R. L. Kavner, and C. M. Lewis, Germanium response to sub-keV nuclear recoils: A multipronged experimental characterization, *Phys. Rev. D* **103**, 122003 (2021).
- [46] L. Li, *A Measurement of The Response of A High Purity Germanium Detector to Low-Energy Nuclear Recoils*, *dissertation*, Duke University (2022).
- [47] G. J. Feldman and R. D. Cousins, Unified approach to the classical statistical analysis of small signals, *Phys. Rev. D* **57**, 3873 (1998).
- [48] J. Neyman, On the problem of confidence intervals, *The Annals of Mathematical Statistics* **6**, 111 (1935).
- [49] A. A. Aguilar-Arevalo *et al.*, Searches for $\text{ce}\nu\text{ns}$ and physics beyond the standard model using skipper-ccds at connie, (2024), [arXiv:2403.15976 \[hep-ex\]](#).
- [50] L. Yang, Y. Liang, and Q. Yue, RECODE program for reactor neutrino CE ν NS detection with PPC Germanium detector, *PoS TAUP2023*, 296 (2024).
- [51] N. Ackermann *et al.*, First observation of reactor antineutrinos by coherent scattering, (2025), [arXiv:2501.05206 \[hep-ex\]](#).